

Magnetic properties of a spin- $\frac{1}{2}$ quadrumer chain

Andreas Honecker and Wolfram Brenig

Institut für Theoretische Physik, TU Braunschweig, Mendelssohnstr. 3, 38106 Braunschweig, Germany.
(September 19, 2000; revised December 23, 2000)

We study a novel $S = 1/2$ cluster chain Hamiltonian which has recently been proposed in the context of the charge ordered low-temperature phase of α' - NaV_2O_5 . We perform a detailed investigation of this model within a large range of parameters using perturbation theory and Lanczos diagonalization. Using model-specific local conservation laws and parameter-dependent mappings to various effective low-energy Hamiltonians we uncover a rich phase diagram and several regimes of gapful spin-excitations. We find that the overall features of recent neutron scattering data on α' - NaV_2O_5 can be fitted within this model, however using a set of parameters which seems unlikely.

PACS numbers: 75.10.Jm, 75.40.-s, 75.40.Mg, 75.50.Ee

I. INTRODUCTION

Low-dimensional magnetic materials exhibit many interesting and sometimes puzzling properties. In particular, the origin of the spin gap in the low-temperature phase of α' - NaV_2O_5 is under intense discussion since it was first reported to open with a phase transition at $T = 34\text{K}$ [1]. It was confirmed soon [2] that this transition is accompanied with a lattice distortion. Charge ordering was also realized to play an important rôle [3], leading to various ordering patterns proposed [4–6]. Recently, based on new determinations of the low-temperature crystal structure [7], two groups [8,9] have proposed a new type of charge ordering which is sketched in Fig. 1. This structure incorporates Vanadium ions in three types of valence states: V^{4+} , V^{5+} and $\text{V}^{4.5+}$. Entering the low-temperature phase below $T = 34\text{K}$, every *second* of the quarter-filled two-leg ladders, which make up the system at high temperatures [10] is in a zig-zag ordered pattern proposed previously for all of the ladders [6]. The remaining ladders survive the transition. This new proposal does not completely rule out other scenarios e.g. with only V^{4+} and V^{5+} since the charges were determined only indirectly through the crystal structure whose determination in itself appears to be delicate [11]. Nevertheless, the charge order proposed by [8,9] is appealing since it contains clusters of six Vanadium ions with a total of four unpaired electrons (indicated by bold lines in Fig. 1) and therefore a spin gap arises naturally [9].

The nature of magnetic excitations above the gap in the low-temperature phase of α' - NaV_2O_5 , *i.e.* the dispersion of $S = 1$ excitations, has been determined by neutron scattering [12–14]: Along the a -direction, two weakly dispersive excitations with an approximate bandwidth of 1meV are observed. In contrast, there is a rather large dispersion along the b -direction [12], with a band rising from around 10meV to at least 40meV [14]. This suggests that a one-dimensional model extending along the b -axis should result in a reasonable first approxima-

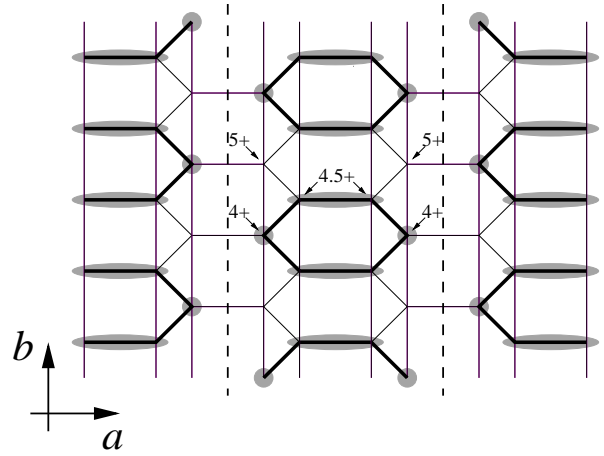


FIG. 1. Possible charge order of Vanadium ions in α' - NaV_2O_5 (schematic). Lines denote the most important (super)exchange paths. The Vanadium atoms are located at intersections and corners; valence states are indicated by the numbers in the center of the figure. Grey shaded areas indicate the localization regime of one unpaired electron. Decoupling along the dashed lines leads to the quadrumer chain.

tion of the magnetic properties. In the charge-ordered state of Fig. 1, this can be implemented by a decoupling along the dashed lines. To leading order in $1/U$ of the related Hubbard model, this leads to the spin- $1/2$ quadrumer chain of Fig. 2 [15].

The properties of the cluster chain model and its relation to α' - NaV_2O_5 are subject to controversial discussion [15,16]. Moreover, not all regimes of parameters possibly relevant to α' - NaV_2O_5 have yet been considered in the literature. In particular, the case $J' < 0$ remains to be investigated as some LDA+U calculations seem to indicate a negative J' [17]. Apart from its possible relevance to α' - NaV_2O_5 , the quadrumer model is closely related to several other interesting spin-chain Hamiltonians [18–21]. Eg., CaV_4O_9 was discussed in the framework of the model in Fig. 2, however with $J_2 = 0$ [18]. The latter

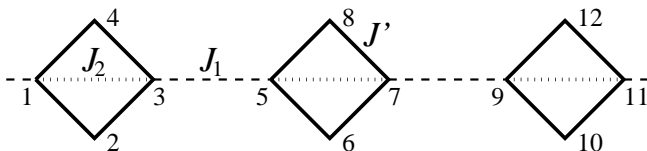


FIG. 2. The quadrumer-chain Hamiltonian. $S = 1/2$ spins are located at the numbered intersection points and corners. Coupling constants are indicated by the style of the lines.

model was also generalized [19] by adding vertical couplings in the quadrumers of Fig. 2. *Local* reflection symmetry of these cluster spin models along the chain direction allows for exact statements regarding the eigenstates and even analytic determination of the ground state in certain parameter regions [19]. Motivated by the preceding, the main goal of this work is to provide an additional careful study of the quadrumer spin-chain combining complementary techniques and enhancing upon the parameter space investigated so far.

The paper is organized as follows: In section II, we describe the quadrumer-chain Hamiltonian more precisely and discuss the limit of decoupled quadrumers. Then we study the inter-quadrumer coupling J_1 perturbatively in section III. We proceed with a numerical analysis of the model in section IV and try to fit the neutron scattering data with this method in section V. Finally, we summarize and discuss our results in section VI. Supplementary results regarding the magnetization process of the quadrumer-chain model are presented in an appendix.

II. PRELIMINARIES

The $S = 1/2$ Heisenberg Hamiltonian corresponding to the model in Fig. 2 reads

$$H = \sum_{x=1}^{L/4} \left\{ H_{\diamond,x} + J_1 \vec{S}_{4x+3} \cdot \vec{S}_{4x+5} \right\} \quad (1)$$

with

$$H_{\diamond,x} = J' \left(\vec{S}_{4x+1} + \vec{S}_{4x+3} \right) \cdot \left(\vec{S}_{4x+2} + \vec{S}_{4x+4} \right) + J_2 \vec{S}_{4x+1} \cdot \vec{S}_{4x+3}. \quad (2)$$

A more conventional parameterization of the dimerized linear chain embedded in Fig. 2 would be $J_1 = (1 - \delta)J$, $J_2 = (1 + \delta)J$. This emphasizes its relation to the quarter-filled two-leg ladders of the high-temperature phase [10] whose low-energy properties are equivalent to spin-1/2 Heisenberg chains. The dimerization is caused by the lattice distortions accompanying the phase transition [7,9]. Consequently, estimates for the coupling constant of an effective Heisenberg chain such as $J \approx 529\text{K} \approx 45\text{meV}$ [22] can be used in the high-temperature phase. Such estimates are not expected to change drastically below the ordering temperature, apart from the dimerization. In particular the coupling along the chain should remain

antiferromagnetic, *i.e.* the physical regime is that with $J_1, J_2 > 0$. In contrast, the physical regime for J' is less clear. Previous investigations of the model (1) have assumed $J' > 0$ [15,16] while, e.g., in [17] a *ferromagnetic* J' of approximately -18meV has been used, focusing however on a different, *i.e.* zig-zag, charge order. We will therefore investigate both signs of J' .

As a first step, we consider the case of decoupled quadrumers, $J_1 = 0$ where the Hamiltonian (1) decomposes into those of individual quadrumers (2). Rewriting the latter as

$$H_{\diamond,x} = \frac{J'}{2} \left(\vec{L}_x^2 - \vec{T}_{A,x}^2 - \vec{T}_{B,x}^2 \right) + \frac{J_2}{2} \left(\vec{T}_{A,x}^2 - \frac{3}{2} \right) \quad (3)$$

with

$$\begin{aligned} \vec{T}_{A,x} &= \vec{S}_{4x+1} + \vec{S}_{4x+3}, \\ \vec{T}_{B,x} &= \vec{S}_{4x+2} + \vec{S}_{4x+4}, \\ \vec{L}_x &= \vec{T}_{A,x} + \vec{T}_{B,x}, \end{aligned} \quad (4)$$

one infers the spectrum for an isolated quadrumer in Table I. The case $J' > 0$ was discussed in detail in [15]. The ground state is a singlet with a gap to $S = 1$ excitations [9] for sufficiently large J' ($J' > J_2/2$). For an illustration of the spectrum see [15]. The presence of a gap, however, is not immediately clear in two other regimes, namely for $J' < -J_2$ where the ground state carries $L_x = 2$ and for $-J_2 < J' < J_2/2$ where it is degenerate between an $L_x = 0$ and $L_x = 1$ representation.

$T_{A,x}$	$T_{B,x}$	L_x	Eigenvalue	Ground state for ($J_2 > 0$)
0	0	0	$-\frac{3}{4}J_2$	$-J_2 < J' < \frac{J_2}{2}$
0	1	1	$-\frac{3}{4}J_2$	$-J_2 < J' < \frac{J_2}{2}$
1	0	1	$\frac{1}{4}J_2$	
1	1	0	$-2J' + \frac{1}{4}J_2$	$\frac{J_2}{2} < J'$
1	1	1	$-J' + \frac{1}{4}J_2$	
1	1	2	$J' + \frac{1}{4}J_2$	$J' < -J_2$

TABLE I. Spectrum of a single quadrumer.

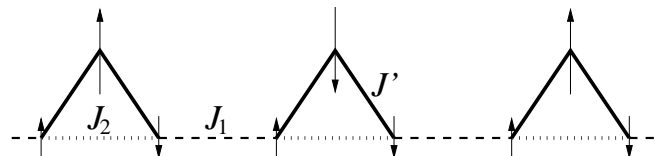


FIG. 3. Effective model for the lowest magnetic excitations. Short arrows denote $S = 1/2$ spins and long ones $S = 1$. Coupling constants are indicated by the style of the lines.

Even if the coupling J_1 is switched on, $T_{B,x}$ remains a good quantum number *locally*, *i.e.* for all x independently. This is related to the fact that local reflections of a single quadrumer at the middle chain are symmetry operations of the model in Fig. 2. Numerical results (see sections IV and V below) show that the lowest magnetic excitations are always in the sector with all

$T_{B,x} = 1$. These states are symmetric with respect to all local reflections of quadruplets along the chain. This finding yields important simplifications in determining the magnon-dispersion since it suffices to retain only the $S = 1$ combination of the two exterior $S = 1/2$ spins of a quadruplet. This leads to an equivalent description in terms of the simplified model sketched in Fig. 3.

III. PERTURBATION THEORY IN J_1

In this section we focus on a perturbative treatment of inter-quadruplet coupling. According to the previous section, there are three regimes with $L_x = 0, 1$ and 2 ground states on each quadruplet. While the gap can be treated by standard non-degenerate perturbation theory in the case of $L_x = 0$, one has to resort to degenerate perturbation theory in all other cases. Here we show that this leads to effective Hamiltonians which also have a gap to magnetic excitations.

A. $J_2/2 < J'$

For $J_1 = 0$ and $J_2/2 < J'$, the ground state carries $T_{A,x} = T_{B,x} = 1$, $L_x = 0$. In order to simplify the discussion, we will also treat J_2 perturbatively, *i.e.* we will consider the regime $J' \gg |J_1|, |J_2|$. Then the lowest excited state is obtained by creating an $T_{A,x_0} = T_{B,x_0} = 1$, $L_{x_0} = 1$ excitation on one quadruplet x_0 . From this we obtain the following third-order expansion in J_1, J_2 of the dispersion

$$\begin{aligned} \frac{\Delta(k)}{J'} = & 1 - \frac{31}{1728}j_1^2 - \frac{1}{768}j_1^3 - \frac{287}{6912}j_1^2j_2 \\ & + \left(\frac{1}{3}j_1 + \frac{7}{72}j_1^2 - \frac{2825}{165888}j_1^3 + \frac{13}{432}j_1^2j_2 \right) \cos(k) \\ & + \left(\frac{1}{108}j_1^2 + \frac{31}{1296}j_1^3 + \frac{5}{162}j_1^2j_2 \right) \cos(2k) \\ & + \frac{13}{1944}j_1^3 \cos(3k) \end{aligned} \quad (5)$$

with

$$j_i = \frac{J_i}{J'}. \quad (6)$$

Eq. (5) agrees with the second-order result derived for $j_2 = 0$ in [18]. One can read off from (5) that the minimum of $\Delta(k)$ is at $k = \pi$ for $j_1 > 0$ and at $k = 0$ for $j_1 < 0$.

Substituting a specific value for k into (5), we can compute two further orders. At $k = 0$ and $k = \pi$ we then find the following fifth-order series for the gap:

$$\begin{aligned} \frac{\Delta(0)}{J'} = & 1 + \frac{1}{3}j_1 + \frac{17}{192}j_1^2 + \frac{403}{20736}j_1^2j_2 + \frac{6109}{497664}j_1^3 \\ & + \frac{1657}{248832}j_1^2j_2^2 + \frac{229}{36864}j_1^3j_2 - \frac{5731}{4976640}j_1^4 \end{aligned}$$

$$\begin{aligned} & + \frac{6763}{2985984}j_1^2j_2^3 + \frac{157691}{71663616}j_1^3j_2^2 \\ & - \frac{29797819}{42998169600}j_1^4j_2 - \frac{1130744639}{1031956070400}j_1^5, \end{aligned} \quad (7)$$

$$\begin{aligned} \frac{\Delta(\pi)}{J'} = & 1 - \frac{1}{3}j_1 - \frac{61}{576}j_1^2 - \frac{845}{20736}j_1^2j_2 + \frac{16403}{497664}j_1^3 \\ & - \frac{6599}{248832}j_1^2j_2^2 - \frac{2959}{995328}j_1^3j_2 + \frac{245833}{9953280}j_1^4 \\ & - \frac{48917}{2985984}j_1^2j_2^3 + \frac{13813}{71663616}j_1^3j_2^2 \\ & + \frac{934164461}{42998169600}j_1^4j_2 - \frac{7289503141}{1031956070400}j_1^5. \end{aligned} \quad (8)$$

The series presented above will be compared to numerical results in section IV and one will see that they are quite accurate in the region where they are valid [23].

B. $-J_2 < J' < J_2/2$

For $-J_2 < J' < J_2/2$, one reads off from Table I that there are two degenerate ground states on each cluster for $J_1 = 0$. Both of them carry $T_{A,x} = 0$, one is a singlet with $T_{B,x} = 0$ and the other one is a triplet with $T_{B,x} = 1$.

In view of the effective spin-model of Fig. 3, only the triplet state with $T_{B,x} = 1$ contributes to the low-energy magnetic excitations for $J_1 \neq 0$. Based on second-order degenerate perturbation theory in J_1 one therefore expects the system to be equivalent to an effective $S = 1$ chain as was already remarked in [15,16]. However, this effective chain is *not* a simple $S = 1$ Heisenberg-chain: While first-order interactions vanish, we find already at second order biquadratic terms which have not been discussed before. Thus, the effective Hamiltonian is

$$\frac{H_{\text{eff}}^{(S=1)}}{J_1^2} = \frac{e_0 L}{4} + \mathcal{J} \sum_{x=1}^{L/4} \left\{ \vec{S}_x \cdot \vec{S}_{x+1} + \beta \left(\vec{S}_x \cdot \vec{S}_{x+1} \right)^2 \right\}, \quad (9)$$

where \vec{S}_x is an effective $S = 1$ operator for the quadruplet x . We have determined the coupling constants in (9) to be

$$\begin{aligned} e_0 = & -\frac{12(J_2 - 3J')J_2^3 + 17(J' + J_2)J_2J'^2 - 8J'^4}{32(J_2 - 2J')(2J_2 - J')(2J_2 - 3J')(J_2 + J')J_2}, \\ \mathcal{J} = & \frac{(4J_2 - J')J'^2}{32(2J_2 - J')(2J_2 - 3J')(J_2 + J')J_2}, \\ \beta = & -\frac{(3J_2 - 2J')J'^2}{2(J_2 - J')(4J_2 - J')(J_2 - 2J')}. \end{aligned} \quad (10)$$

These effective coupling constants are shown in Fig. 4 for the region where the mapping applies. One finds that \mathcal{J} is always positive (antiferromagnetic) while β is always negative. At the boundaries of the figure, we have the following divergences: $\mathcal{J} \rightarrow \infty$ as $J' \rightarrow -J_2$ and $\beta \rightarrow -\infty$ as $J' \rightarrow J_2/2$. These divergences are expected since

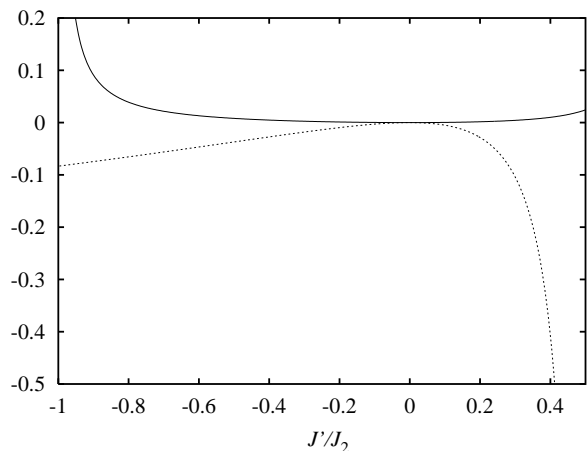


FIG. 4. Coupling constants for the effective biquadratic $S = 1$ chain: The lines denote $\mathcal{J} \times J_2$ (full) and β (dotted).

they signal the limit of validity of the mapping to an effective $S = 1$ chain.

The effective Hamiltonian (9) with coupling constants (10) is gapful with the exception of $J' = 0$ and $J' \approx 0.4466J_2$ (corresponding to $\beta = -1$ – see for instance Sec. 6 of [24]). The ground state is the Haldane phase for $-J_2 < J' \lesssim 0.4466J_2$ and it is spontaneously dimerized only in the small window $0.4466J_2 \lesssim J' < J_2/2$ (see Sec. 6 of [24]). Interestingly though, the latter window includes the region presumably most relevant to α' - NaV_2O_5 , which we will find to be $J' \approx J_2/2$ (see section V below). The biquadratic term thus has the important consequence that the relevant parameter region of the quadrumer chain is not adjacent to a Haldane state, but to a dimerized state.

Regarding the size of the gap obtained by this mapping, one observes that \mathcal{J} is very small in most of the region covered by Fig. 4. For example, for $-0.7264J_2 < J' < J_2/2$, we have $J_2 \times \mathcal{J} < 1/40$. In combination with the additional factor J_1^2 this leads to an extremely small gap of the original Hamiltonian at least in the region $J_1 \ll J_2$ where the perturbative approach is valid.

C. $J' < -J_2$

Finally, for $J' < -J_2$ and $J_1 = 0$, the ground state of each quadrumer is an $L_x = 2$ representation. Using first-order degenerate perturbation theory in J_1 , the quadrumer chain can then be mapped to an effective $S = 2$ Heisenberg chain

$$H_{\text{eff.}}^{(S=2)} = \frac{J_1}{16} \sum_{x=1}^{L/4} \vec{S}_x \cdot \vec{S}_{x+1}, \quad (11)$$

where now \vec{S}_x is an effective $S = 2$ operator for the quadrumer x . The gap of the effective $S = 2$ chain was estimated by DMRG to be $\Delta_{\text{eff.}} = (0.0876 \pm 0.0013)J_{\text{eff.}}$ [25]. Substitution of $J_{\text{eff.}} = J_1/16$ into this DMRG result

then leads to a small, but non-zero gap of the quadrumer model

$$\Delta \approx 0.0055J_1 + \mathcal{O}(J_1^2) \quad (12)$$

for $J' < -J_2$ and weakly antiferromagnetic $J_1 > 0$.

IV. LANCZOS DIAGONALIZATION

We now proceed to study the spin gap over a wider range of parameters using Lanczos diagonalization. We have used periodic boundary conditions and mostly worked with the original model (1), only for the case of $L = 32$ spin-1/2 spins have we resorted to the effective Hamiltonian of Fig. 3 to reduce the dimensionality of the Hilbert space.

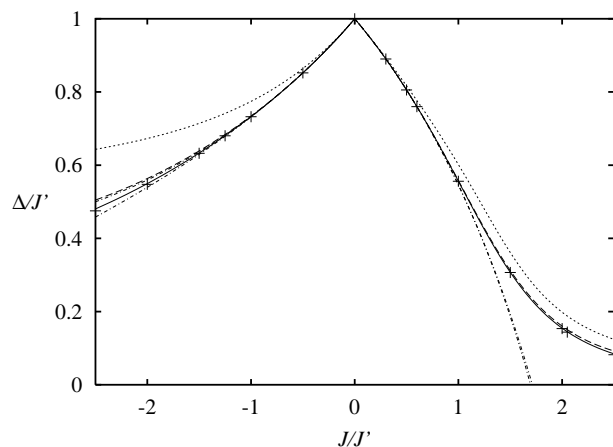


FIG. 5. Spin gap as a function of $J = J_1 = J_2$ for $J' > 0$. Lines are for $L = 8$ (dotted), $L = 16$ (dashed) and $L = 24$ (full). The symbols ‘+’ denote an extrapolation to the thermodynamic limit and the dashed-dotted lines [2,3] and [3,2] Padé approximants to the series (7) for $J < 0$ and (8) for $J > 0$.

We begin with parameters that permit a comparison with perturbative results of the previous section. Fig. 5 shows the spin gap, *i.e.* the minimum of the one-magnon dispersion, as a function of J for $J' > 0$ and a homogeneous chain with $J = J_1 = J_2$, including the region $|J| \ll J'$ where perturbation theory should be accurate. In this figure, we show numerical data for $L = 8, 16$ and 24 . Actually, we have determined the lowest excitations in the $S^z = 1$ sector, but we are confident that this is in fact always an excitation with total spin $S = 1$. The finite-size data was extrapolated with a Shanks transformation [26], yielding the pluses in Fig. 5. These extrapolations are indistinguishable from the $L = 24$ data, showing that finite-size effects are extremely small at least for the parameters covered by the figure.

Recall that eq. (5) shows that the minimum of the one-magnon dispersion is located at $k = 0$ for $J < 0$ and at $k = \pi$ for $J > 0$. This is confirmed by our numerical data.

Therefore, one should compare the numerical data to the series (7) and (8) for $J < 0$ and $J > 0$, respectively. Padé approximants to these series are shown in Fig. 5 and one observes good agreement for $|J| \lesssim J'$. While the approximants stay close to the numerical data for negative J as large as $J = -2.5J'$, systematic deviations are observed at large positive J . This can be attributed to the fact that other $S = 1$ excitations start to mix in at $J' \approx J$ (compare Table I and [16]).

As a first summary, we find good agreement between our numerical data and perturbation theory in the regime where the latter should be accurate. For $J \gtrsim J'$, however, the numerical approach is far superior since the nature of the lowest $S = 1$ excitation becomes more complicated. Yet, finite-size effects still remain small.

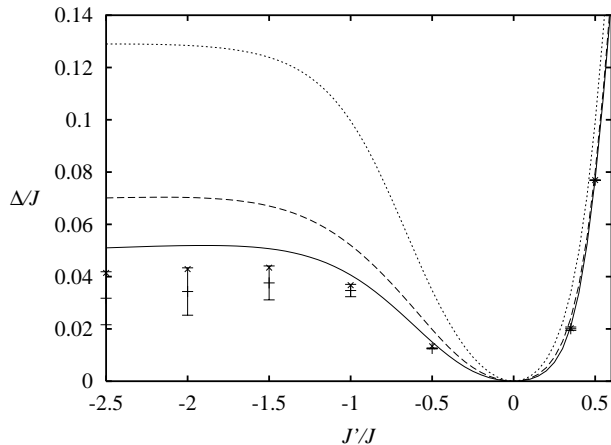


FIG. 6. Same as Fig. 5, but now as a function of J' for $J > 0$. The symbols ‘x’ denote $L = 32$ data and a ‘+’ with error bars an extrapolation to the thermodynamic limit.

We now concentrate on the region $J > 0$, *i.e.* the one which is appropriate for α' - NaV_2O_5 , and study the dependence on J' , focusing on small and negative values. Fig. 6 again shows the spin gap, now as a function of J' for $J = J_1 = J_2 > 0$. The extrapolations have again been performed with a Shanks transformation [26]. The actual estimate is based on the $L = 16, 24$ and 32 data with error bars determined from the difference with respect to an extrapolation based on $L = 8, 16$ and 24 . For $J' > 0$, the trend observed in Fig. 5, *i.e.* that $L = 8, 16$ and 24 is completely sufficient for the extrapolation, is confirmed. For $J' < 0$ and small, the errors first remain small with an increasing uncertainty as J' becomes large and negative. Larger error bars indicate larger finite-size effects which in turn originate from an increasing correlation length.

Fig. 5 shows that the gap vanishes at $J' = 0$ at any finite system size, the reason being that the exterior spins are free in this case and give rise to excitations with exactly zero energy. For any non-zero J' , in contrast, the gap seems to remain non-zero even in the thermodynamic limit.

A maximum of Δ/J emerges in the ferromagnetic re-

gion $-2J \lesssim J' \lesssim -J$. In fact, while Δ/J is already of the correct order of magnitude, it still has to decrease substantially for $J' \rightarrow -\infty$ in order to reach the value given by (12). In the limit $J' \rightarrow -\infty$, we also have to recover the correlation length ξ of the $S = 2$ chain which is known to be $\xi \approx 50$ clusters (*i.e.* $L \approx 200$ – see for example [27]), thus leading to the increasing finite-size effects in Fig. 6 as J' goes to larger negative values.

In the region of positive $J, J' > 0$, our results can be compared to DMRG results (see Fig. 2 of [15]). While we find agreement for large J' , deviations of the order of $J/50$ can be observed in the region of small J' . For instance, we extrapolate a gap $\Delta \approx 0.077J$ for $J' = 0.5J$ while the corresponding value of [15] is $\Delta \approx 0.05J$. Furthermore, the DMRG result of [15] for the gap is essentially zero already for $J' = 0.4J$ while our extrapolation at $J' = 0.35J$ yields $\Delta = 0.0201(6)J$ which is clearly non-zero. This discrepancy can be observed already at a fixed system size (e.g. $L = 32$) [28], *i.e.* it is not due to the extrapolation. There are two main distinctions between our Lanczos and the DMRG results of [15]: First, DMRG is subject to truncation errors which are absent in our approach. Second, we use periodic boundary conditions in contrast to open ones in [15]. Periodic boundary conditions typically have smaller finite-size effects than open ones and open boundary conditions can even lead to further boundary excitations. We therefore believe that extrapolation of our Lanczos data for system sizes up to $L = 32$ yields the most accurate results obtained so far for the thermodynamic limit of the model (1).

V. FITTING THE NEUTRON SCATTERING DATA

We have seen so far that there are several regions where different mechanisms open a spin gap in the quadrumer-chain model with a large variation of its size. While this looks promising for the applicability of the model to α' - NaV_2O_5 , the real test is whether the neutron-scattering results for the dispersion along the b -axis [12,14] can be fitted with reasonable parameters.

Here we follow [15] and use the following criteria: (i) The low-temperature experimental data [12,14] has a minimum in the center of the high-temperature Brillouin zone. Taking into account doubling of the unit cell (as is appropriate for the quadrumer-chain model), the minimum of the dispersion should therefore be located at $k = 2\pi \equiv 0$ and should have a value $\Delta(0) \approx 10\text{meV}$. (ii) Since the magnon dispersion was recently traced up to energies of 40meV [14], one should have $\Delta(\pi) \geq 40\text{meV}$.

In Figs. 7a),b) we first show the dispersion of the lowest $S = 1$ excitation corresponding to the two points $J' = \pm J/2$ in Fig. 6. One observes that the minimum is located at $k = \pi$ and remains there after extrapolation to the thermodynamic limit. Fig. 7c) shows the dispersion for $J' = 0.65J_2$ and a small dimerization $\delta \approx 0.053$

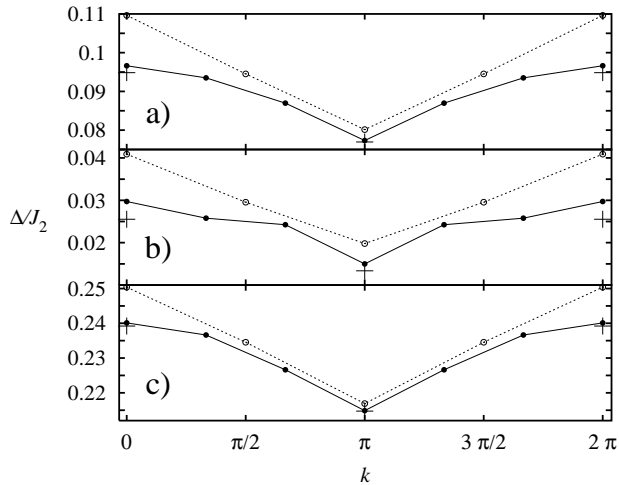


FIG. 7. Dispersion of lowest $S = 1$ excitation for a) $J_1 = J_2 = 2J'$, b) $J_1 = J_2 = -2J'$ and c) $J_1 = 0.9J_2$, $J' = 0.65J_2$. Symbols are for $L = 16$ (open circles), $L = 24$ (filled circles) and $L = 32$ (pluses). Lines are guides to the eye.

which is close to a parameter set proposed as a possible fit for α' - NaV_2O_5 in [16]. One observes that our data is already well converged with system size and one can thus easily extrapolate it to $L = \infty$. We find $\Delta(0) \approx 0.239J_2$, which agrees with [16], but the minimum is still at $k = \pi$: $\Delta(\pi) \approx 0.215J_2$, leading to $\Delta(\pi)/\Delta(0) \approx 0.9$. We therefore agree with [15] that this parameter region is *not* appropriate for α' - NaV_2O_5 .

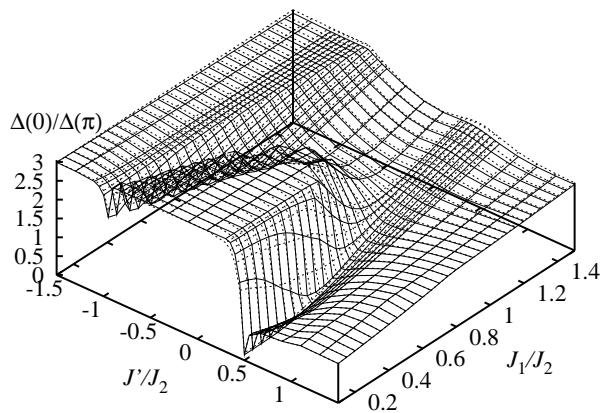


FIG. 8. $\Delta(0)/\Delta(\pi)$ as a function of coupling to external spins J'/J_2 and coupling between quadrumers J_1/J_2 for $L = 16$ (dotted lines) and $L = 24$ (full lines).

In order to test whether a good fit can be obtained at all, we have performed a systematic numerical scan of $\Delta(0)/\Delta(\pi)$ at $L = 16$ and $L = 24$. The range of interest including ferromagnetic couplings $J' < 0$ we find, is depicted in Fig. 8. Apart from this range we have also studied a wide region of J'/J_2 and J_1/J_2 . We found little variation outside the parameter window shown in Fig. 8. Note that $\Delta(k)$ was determined for $S^z = 1$ excitations

which do not necessarily carry $S = 1$, but may have higher spin. Furthermore, there should be a two-particle state at $k = 0$ with an energy not larger than $2\Delta(\pi)$ in the thermodynamic limit. The ratio $\Delta(0)/\Delta(\pi)$ should therefore not exceed a value of 2 in the thermodynamic limit unless the gap closes. This indicates large finite size effects in some regions of Fig. 8. However, we are interested in parameters where $\Delta(0)/\Delta(\pi) < 1$. In that case no complications due to multi-magnon excitations are expected.

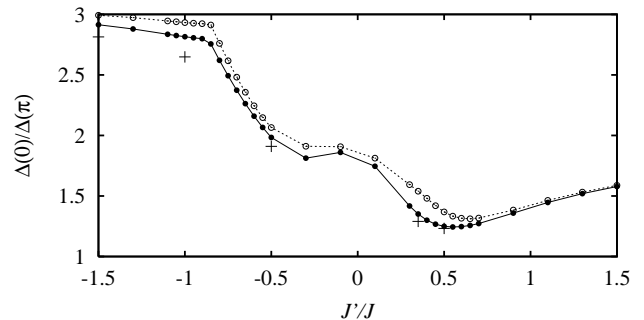


FIG. 9. $\Delta(0)/\Delta(\pi)$ for $J_1 = J_2 = J$ as a function of J' for $L = 16$ (open circles), $L = 24$ (filled circles) and $L = 32$ (pluses). Lines are guides to the eye.

For clarity, Fig. 9 shows a section along $J_1 = J_2$ of Fig. 8 including some $L = 32$ data points (compare also Figs. 7a),b)). One observes that finite-size effects can be important, in particular for $J' < 0$ where $\Delta(0)/\Delta(\pi)$ exceeds the aforementioned limiting value of two. It is evident from this figure that finite-size effects reduce $\Delta(0)/\Delta(\pi)$. The condition $\Delta(0) < \Delta(\pi)$ appears nevertheless impossible to satisfy at $J_1 = J_2$. Moreover, in the entire region with $J' < 0$, Fig. 8 clearly shows that $\Delta(0)$ is always larger than $\Delta(\pi)$, restricting the possible parameters for a fit to lie in the region $J' > 0$. This is consistent with refs. [15,16].

On the other hand, there is a narrow region around $J' = J_2/2$ with $J_1 < J_2$ where $\Delta(0)$ becomes smaller than $\Delta(\pi)$. An example of an excitation spectrum in this region is shown in Fig. 10. One does indeed see a single magnon excitation with a minimum at $k = 0$ whose dispersion is interpolated by the full line. This dispersion would be consistent with early neutron scattering data [12]. However, very recent measurements [14] clearly show that the bandwidth in Fig. 10 is too small. One may obtain a larger bandwidth within the present model by changing the coupling constants slightly, however, only at the expense of reducing $\Delta(0)$. In order to have $\Delta(0) = 10\text{meV}$ and $\Delta(\pi) \geq 40\text{meV}$ one then needs a coupling constant $J = J_2/(1 + \delta) \gtrsim 300\text{meV}$ with a dimerization $\delta \approx 0.38 \dots 0.54$ and $J' \approx (0.5 \dots 0.55)J_2$ [29]. Both, the large values of J and of the dimerization are certainly too large to be plausible (see section II). Therefore, even though our numerical results differ in detail we agree with [15] regarding that the cluster spin model (1) does not result in a quantitative fit for α' - NaV_2O_5 with

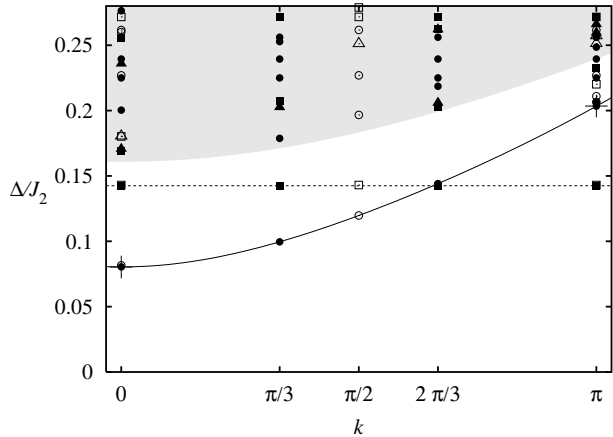


FIG. 10. Low-lying excitations at $J_1/J_2 = 7/20$, $J'/J_2 = 11/20$. Open symbols denote data for $L = 16$ and filled symbols for $L = 24$. Boxes stand for $S = 0$ excitations, circles for $S = 1$ excitations and triangles for $S = 2$ excitations. The pluses show the lowest $S = 1$ excitations for $L = 32$ at $k = 0$ and π . The full line denotes the lowest $S = 1$ excitation (magnon) whereas the dashed line shows the lowest, non-dispersive $S = 0$ excitation. The shaded area indicates the expected location of the two-magnon continuum.

plausible parameters.

Among the remaining excitations displayed in Fig. 10, there is a localized (k -independent) singlet with $\Delta(k) \approx 0.14J_2$ (indicated by the dashed line). This excitation can be interpreted as a singlet $T_{B,x_0} = 0$ in one quadrumer x_0 (while all other $T_{B,x} = 1$) which is prevented from propagating since $T_{B,x}$ is locally conserved. Note that such excitations are not present in the effective model of Fig. 3, but only in the original one of (1).

We would like to conclude this section with a remark on Fig. 8: There is one dip in $\Delta(0)/\Delta(\pi)$ for $J_1 < J_2$ both for negative and positive J' . These dips become sharp for $J_1 \rightarrow 0$ where they signal transitions between different local ground states. In this limit, the dips are located at $J'/J_2 = -1$ and $J'/J_2 = 1/2$ where according to Table I the transitions occur at $J_1 = 0$. In general, our numerical data is consistent with a vanishing gap at the location of these dips, *i.e.* a continuous transition between different phases. However, due to the large correlation lengths expected in some of the phases, larger system sizes would be needed in order to determine the phase diagram of the model (1) accurately.

VI. CONCLUSIONS AND OUTLOOK

We have studied an $S = 1/2$ quadrumer-chain model using perturbation theory and the Lanczos method. This model has been proposed to explain the magnetic excitations of α' - NaV_2O_5 in its low-temperature phase [8,9,15]. We have shown the quadrumer-chain Hamiltonian to dis-

play a rich phase diagram which we believe the present study has just begun to unveil (compare Fig. 8): Different phases are smoothly connected to the local $L_x = 0, 1$ and 2 ground states at $J_1 = 0$. In addition, the mapping to an effective $S = 1$ chain in section III B shows that the $L_x = 1$ region consists of a Haldane and a dimerized phase at least at small J_1 . The latter phase arises because of a biquadratic interaction which has not been realized in previous studies. However, further work is needed to determine all of the phase boundaries of the quadrumer chain accurately.

The model (1) gives also rise to interesting behavior in an external magnetic field. The case $J_1 = J_2$ is discussed in an appendix where we show that in addition to a spin gap one also finds a plateau in the magnetization curve at half the saturation magnetization. This is similar as for the model studied in [21], though it remains to be investigated whether one can also obtain other plateaux in the present model for $J_1 \neq J_2$ like the one at a quarter of the saturation magnetization found in [21].

Finally, we have assessed the relevance of the quadrumer-chain model to the magnetic excitations of α' - NaV_2O_5 . We found that in order to fit the neutron scattering data for the dispersion along the chain direction [14] one has to resort to parameters which are not very plausible. A good fit can even be obtained for $J_i < 0$, (compare (5) and Fig. 5) although ferromagnetic exchange along the chain is clearly an unphysical choice. The applicability of the quadrumer model to α' - NaV_2O_5 may therefore be questioned [15], leaving the proper microscopic model for this material an open issue. In fact, other models proposed in this context are similarly deficient. Assuming, e.g., pure zig-zag charge order [6], the lowest $S = 1$ excitation would belong to a two-particle continuum (see, e.g., [30]) rather than the experimentally observed magnon state [12,14]. A possible remedy is to attribute the spin gap to dimerization [31] rather than frustration. However, this proposal has been disputed [16] based on the spatial symmetries of the charge ordered state. Clearly, further experimental input is needed to decide these issues. For the moment, we cannot rule out that the correct description of α' - NaV_2O_5 will turn out to be a modification of the cluster model discussed in the present work.

ACKNOWLEDGMENTS

We would like to thank T. Chatterji and C. Gros for relevant discussions and correspondence. This work has benefited from the Schwerpunkt 1073 of the Deutsche Forschungsgemeinschaft.

APPENDIX: MAGNETIZATION PROCESS

In this appendix we discuss the magnetization process of the quadrumer-chain model at $J_1 = J_2 = J$. Application of an external magnetic field amounts to adding a term $-h \sum_{x=1}^L S_x^z$ to the Hamiltonian (1). We have computed the magnetization curve numerically for $L \leq 32$ (as one example, the magnetization curve for $J = J'$ is shown in the inset of Fig. 11) and then extrapolated it to the thermodynamic limit. The final result is shown in Fig. 11. First, we find an $\langle M \rangle = 0$ plateau which is equivalent to the spin gap (accordingly, its boundary curve in Fig. 11 is equivalent to Fig. 5). In addition, we find a clear plateau at $\langle M \rangle = 1/2$ (in a normalization where the fully polarized state has $\langle M \rangle = 1$). Such a plateau is expected on the basis of the limit of decoupled quadrumers (2) – see [32] and references therein. Similar behavior has been observed for the related model of ref. [19] where an interesting sequence of magnetization plateaux was found [21]. One remarkable feature of the present model is that there is evidence for a transition in the $\langle M \rangle = 1/2$ plateau state at $J \approx 0.65J'$.

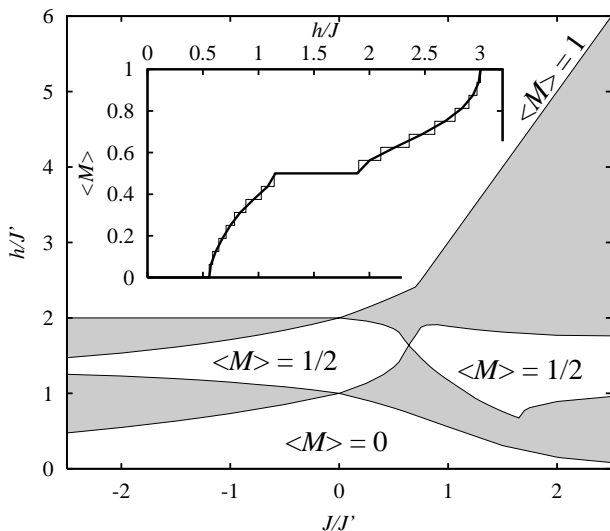


FIG. 11. Groundstate phase diagram in a magnetic field h for $J_1 = J_2 = J$. White areas denote parameter regions with magnetization plateaux with the indicated values of the magnetization $\langle M \rangle$ whereas the grey shaded regions denote smooth transitions. Inset: Magnetization curve at $J' = J$ for $L = 32$ (thin line) and an extrapolation to the thermodynamic limit (bold line).

[1] M. Isobe, Y. Ueda, J. Phys. Soc. Jpn. **65**, 1178 (1996).
 [2] Y. Fujii, H. Nakao, T. Yoshihama, M. Nishi, K. Nakajima,

K. Kakurai, M. Isobe, Y. Ueda, H. Sawa, J. Phys. Soc. Jpn. **66**, 326 (1997).
 [3] T. Ohama, H. Yasuoka, M. Isobe, Y. Ueda, Phys. Rev. **B59**, 3299 (1999).
 [4] T. Chatterji, K.D. Liß, G.J. McIntyre, M. Weiden, R. Hauptmann, C. Geibel, Solid State Commun. **108**, 23 (1998).
 [5] P. Thalmeier, P. Fulde, Europhys. Lett. **44**, 242 (1998).
 [6] H. Seo, H. Fukuyama, J. Phys. Soc. Jpn. **67**, 2602 (1998); M.V. Mostovoy, D.I. Khomskii, Solid State Commun. **113**, 159 (1999).
 [7] J. Lüdecke, A. Jobst, S. van Smaalen, E. Morr e, C. Geibel, H.-G. Krane, Phys. Rev. Lett. **82**, 3633 (1999).
 [8] S. van Smaalen, J. Lüdecke, Europhys. Lett. **49**, 250 (2000).
 [9] J.L. de Boer, A. Meetsma, J. Baas, T.T.M. Palstra, Phys. Rev. Lett. **84**, 3962 (2000).
 [10] H. Smolinski, C. Gros, W. Weber, U. Peuchert, G. Roth, M. Weiden, C. Geibel, Phys. Rev. Lett. **80**, 5164 (1998).
 [11] J.L. de Boer, G. Maris, A. Meetsma, J. Baas, T.T.M. Palstra, preprint cond-mat/0008054.
 [12] T. Yoshihama, M. Nishi, K. Nakajima, K. Kakurai, Y. Fujii, M. Isobe, C. Kagami, Y. Ueda, J. Phys. Soc. Jpn. **67**, 744 (1998).
 [13] L.-P. Regnault, J.E. Lorenzo, J.-P. Boucher, B. Grenier, A. Hiess, T. Chatterji, J. Jegoudez, A. Revcolevschi, Physica **B276-278**, 626 (2000).
 [14] B. Grenier, O. Cepas, L.P. Regnault, J.E. Lorenzo, T. Ziman, J.P. Boucher, A. Hiess, T. Chatterji, J. Jegoudez, A. Revcolevschi, preprint cond-mat/0007025.
 [15] C. Gros, R. Valent ı, J.V. Alvarez, K. Hamacher, W. Wenzel, Phys. Rev. **B62**, R14617 (2000).
 [16] S. Trebst, S. Sengupta, Phys. Rev. **B62**, R14613 (2000).
 [17] P. Thalmeier, A.N. Yaresko, Eur. Phys. J. **B14**, 495 (2000).
 [18] N. Katoh, M. Imada, J. Phys. Soc. Jpn. **64**, 4105 (1995).
 [19] N.B. Ivanov, J. Richter, Phys. Lett. **A232**, 308 (1997); J. Richter, N.B. Ivanov, J. Schulenburg, J. Phys.: Condensed Matter **10**, 3635 (1998).
 [20] A. Koga, S. Kumada, N. Kawakami, T. Fukui, J. Phys. Soc. Jpn. **67**, 622 (1998).
 [21] A. Koga, K. Okunishi, N. Kawakami, Phys. Rev. **B62**, 5558 (2000).
 [22] F. Mila, P. Millet, J. Bonvoisin, Phys. Rev. **B54**, 11925 (1996).
 [23] Besides the excitation considered in the present section, there is another low-lying excitation which becomes the lowest excited state for $J_2/2 < J' < J_2$ and $J_1 = 0$ (see Table I). Perturbative expansions for both excitations were performed numerically in [16].
 [24] I. Affleck, Nucl. Phys. **B265**, 409 (1986).
 [25] Xiaoqun Wang, Shaojing Qin, Lu Yu, Phys. Rev. B **60**, 14529 (1999).
 [26] D. Shanks, J. Math. and Phys. **34**, 1 (1955).
 [27] Y.J. Kim, M. Greven, U.-J. Wiese, R.J. Birgeneau, Eur. Phys. J. B **4**, 291 (1998).
 [28] C. Gros, private communication.
 [29] We were unable to reproduce the best fit of [15]: $\delta = 0.2$, $J \approx 126\text{meV}$. Indeed, it was pointed out in [15] that the cluster-operator theory on which this fit was based is not

accurate in the region of interest.

- [30] B.S. Shastry, B. Sutherland, Phys. Rev. Lett. **47**, 964 (1981).
- [31] C. Gros, R. Valentí, Phys. Rev. Lett. **82**, 976 (1999).
- [32] D.C. Cabra, M.D. Grynberg, A. Honecker, P. Pujol, preprint cond-mat/0010376.